13

Wave Field Synthesis Techniques for Spatial Sound Reproduction

Rudolf Rabenstein, Sascha Spors, and Peter Steffen

Telecommunications Laboratory, University Erlangen-Nuremberg, Germany

13.1 Introduction

Wave field synthesis (WFS) is a sound reproduction technique which overcomes certain limitations of conventional surround sound methods. It is based on a physical description of the propagation of acoustic waves. Wave field synthesis uses loudspeaker array technology to correctly reproduce sound fields without the "sweet spot" limitation well-known from stereophonic surround sound methods.

The main applications of wave field synthesis are in the areas of entertainment and the performing arts. Due to its rigorous physical foundations, wave field synthesis is also used for reproduction of sound fields caused by room reverberation or for the creation of virtual noise fields. It may not only recreate sound fields of virtual theaters and concert halls, but also acoustic environments for human communication. This way, wave field synthesis provides acoustical testbeds for echo and noise control solutions.

Wave field synthesis techniques are formulated in terms of the acoustic wave equation and the description of its solutions by Green's functions. These foundations have been initially developed by the Technical University of Delft [3, 6, 11, 18, 22–25] and were later extended within the European project CARROUSO [5].

This chapter discusses the signal processing aspects of state-of-the-art wave field synthesis systems. The most important of these aspects is the generation of the correct driving signals for each loudspeaker by suitable digital signal processing. Sec. 13.2 presents the notation and some elements from the foundations of acoustics. They are required for the presentation of the concept of wave field synthesis and the resulting signal processing structure in Sec. 13.3. Finally, an implementation example is given in Sec. 13.4.

13.2 Elements from the Foundations of Acoustics

This section starts with a review of some elements from the foundations of acoustics. At first the notation of the required coordinate systems is presented. Then follows a short discussion of the acoustical wave equation and the representation of its solutions in terms of plane waves and Green's functions. Finally the Kirchhoff-Helmholtz integral is introduced for later reference. These foundations of acoustics and wave physics are found in more detail e.g. in [4, 8, 14, 16, 26].

13.2.1 Coordinate Systems

The correct description of sound propagation in space requires a three-dimensional (3D) formulation of the respective acoustical processes. On the other hand, in many applications the source and receiver positions are located in a plane, e.g. a horizontal plane at the height of the listeners' ears. In these cases, a two-dimensional (2D) description is appropriate. The notation for 2D and 3D coordinates is shown in Fig. 13.1 and is introduced below.

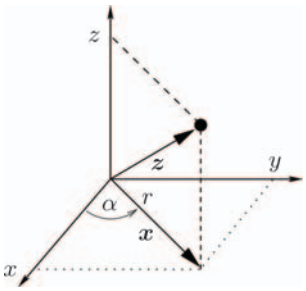

Fig. 13.1. Illustration of Cartesian and polar coordinates.

13.2.1.1 Two-Dimensional Coordinates

Cartesian and polar coordinates in two dimensions are denoted by

$$\boldsymbol{x} = \begin{bmatrix} x \\ y \end{bmatrix}, \qquad \boldsymbol{r} = \begin{bmatrix} r \\ \alpha \end{bmatrix}. \tag{13.1}$$

Their components are related by

$$\begin{bmatrix} x \\ y \end{bmatrix} = r \begin{bmatrix} \cos\alpha \\ \sin\alpha \end{bmatrix}, \qquad \begin{bmatrix} r \\ \alpha \end{bmatrix} = \begin{bmatrix} \sqrt{x^2 + y^2} \\ \tan^{-1}\left(\frac{x}{y}\right) \end{bmatrix}. \tag{13.2}$$

The 2D volume elements used for integration are

$$d\boldsymbol{x} = dx\, dy\,, \qquad d\boldsymbol{r} = r\, dr\, d\alpha\,. \tag{13.3}$$

13.2.1.2 Three-Dimensional Coordinates

The position vector $\boldsymbol{z}$ in Cartesian coordinates is defined as

$$\boldsymbol{z} = \begin{bmatrix} \boldsymbol{x} \\ z \end{bmatrix} = \begin{bmatrix} x \\ y \\ z \end{bmatrix} . \tag{13.4}$$

The volume element for 3D integration is

$$d\boldsymbol{z} = dx\, dy\, dz . \tag{13.5}$$

The assignment $p_0(\boldsymbol{z}) = p_1(\boldsymbol{x})$ means that $p_0(\boldsymbol{z})$ is independent of the z-coordinate.

13.2.2 The Wave Equation

The *wave equation* is given by [14, 16, 26]

$$\Delta p(t, \boldsymbol{z}) - \frac{1}{c^2} \frac{\partial^2}{\partial t^2}\, p(t, \boldsymbol{z}) = 0 . \tag{13.6}$$

$p(t, \boldsymbol{z})$ is the sound pressure at time t and at the location $\boldsymbol{z}$. $\Delta = \nabla^2$ denotes the Laplace operator [2, 9, 10], i.e. second order spatial derivation and c is the propagation speed. Possible solutions of the wave equation are constrained to signals with equal second order partial derivatives in time and space. Solutions of the wave equation are also called *wave fields* or *sound fields*.

Application of the Fourier transform with respect to time turns the wave equation into the *Helmholtz equation*

$$\Delta P(\omega, \boldsymbol{z}) + \left(\frac{\omega}{c}\right)^2 P(\omega, \boldsymbol{z}) = 0 . \tag{13.7}$$

Here the differentiation theorem of the Fourier transform has been applied to substitute the second order time derivative in (13.6) by $(j\omega)^2$ in (13.7). The validity of the conditions for the application of the differentiation theorem have been tacitly assumed. The relation between the temporal frequency variable ω and the propagation speed c is frequently called the wave number $k = \omega/c$.

13.2.2.1 Plane Wave Solution

A *plane wave* is a special solution of the wave equation, which has a very simple form for Cartesian coordinates. It is determined by its wave form and by the direction from which the wave form emanates. The wave form is given by a time function $f(t, \theta)$ and the direction is given by the unit vector $\boldsymbol{n}_\theta$. Later, only plane waves with a zero component in the z-direction are considered. Then $\boldsymbol{n}_\theta$ is a vector in the xy-plane and it is uniquely determined by its x- and y-components

$$\boldsymbol{n}_\theta = \begin{bmatrix} \cos\theta \\ \sin\theta \end{bmatrix} . \tag{13.8}$$

The plane wave solution of Eq. 13.6 is the 3D signal

$$p(t, \boldsymbol{x}) = f\left(t + \frac{1}{c}\langle \boldsymbol{x}, \boldsymbol{n}_\theta \rangle, \theta\right) , \tag{13.9}$$

where $\langle \boldsymbol{x}, \boldsymbol{n}_\theta \rangle$ is the scalar product between $\boldsymbol{x}$ and $\boldsymbol{n}_\theta$. It describes a planar wave front which propagates through space from the direction of $\boldsymbol{n}_\theta$ with speed c. In the origin $\boldsymbol{x} = \boldsymbol{0}$, the wave form $f(t, \theta)$ is observed directly as $p(t, \boldsymbol{0}) = f(t, \theta)$. The Fourier transform with respect to time gives

$$P(\omega, \boldsymbol{x}) = F(\omega, \theta)\, e^{j\frac{\omega}{c}\langle \boldsymbol{x}, \boldsymbol{n}_\theta \rangle} \tag{13.10}$$

as the plane wave solution of Eq. 13.7.

A more general wave field is obtained by superposition of plane wave solutions from all possible directions θ

$$P(\omega, \boldsymbol{r}) = \int_0^{2\pi} F(\omega, \theta)\, e^{j\frac{\omega}{c} r \cos(\theta - \alpha)}\, d\theta , \tag{13.11}$$

where the scalar product $\langle \boldsymbol{x}, \boldsymbol{n}_\theta \rangle$ has been expressed in polar coordinates

$$\langle \boldsymbol{x}, \boldsymbol{n}_\theta \rangle = r \cos(\theta - \alpha) . \tag{13.12}$$

The relation 13.11 is closely related to the plane wave decomposition of a wave field [12].

13.2.2.2 Green's Functions

Arbitrary solutions of the wave equation with homogeneous boundary conditions are described in terms of Green's functions. They can be regarded as the response of a sound field to an impulse in time and space. Since there are various kinds of impulse functions in 3D space, also the possible forms of the corresponding Green's functions differ. Here, the Green's functions of point sources and line sources are considered.

Point Source

A point source in 3D space is defined by the 3D Dirac-impulse function in Cartesian coordinates [4, 8]

$$\delta_{3\mathrm{D}}(\boldsymbol{z}) = \delta(x)\, \delta(y)\, \delta(z) , \tag{13.13}$$

where $\delta(x)$ denotes the 1D Dirac-impulse. The 3D Dirac-impulse can also be defined for cylindrical and other 3D coordinates. A point source at the location $\boldsymbol{z}'$ with time varying source strength is described by

$$q_0(t, \boldsymbol{z}) = q_0(t, \boldsymbol{z}')\, \delta_{3\mathrm{D}}(\boldsymbol{z} - \boldsymbol{z}') \tag{13.14}$$

or after Fourier transform with respect to time by

$$Q_0(\omega, \boldsymbol{z}) = Q_0(\omega, \boldsymbol{z}')\, \delta_{3\mathrm{D}}(\boldsymbol{z} - \boldsymbol{z}')\,. \tag{13.15}$$

The index zero indicates a point sources with dimension zero. An arbitrary spatial distribution of point sources is given by

$$Q_0(\omega, \boldsymbol{z}) = \iiint\limits_V Q_0(\omega, \boldsymbol{z}')\, \delta_{3\mathrm{D}}(\boldsymbol{z} - \boldsymbol{z}')\, d\boldsymbol{z}'\,. \tag{13.16}$$

The spatial sound field $P_0(\omega, \boldsymbol{z})$ caused by a spatially distributed source $Q_0(\omega, \boldsymbol{z})$ is given by

$$P_0(\omega, \boldsymbol{z}) = \iiint\limits_V G_0(\omega, \boldsymbol{z}|\boldsymbol{z}')\, Q_0(\omega, \boldsymbol{z}')\, d\boldsymbol{z}'\,. \tag{13.17}$$

The Green's function $G_0(\omega, \boldsymbol{z}|\boldsymbol{z}')$ describes the contribution of a point source at position $\boldsymbol{z}'$ to the sound field at position $\boldsymbol{z}$. The integration is carried out on the volume V where the solution of the wave equation is considered. The position $\boldsymbol{z}$ is also referred to as the listener position.

The form of the Green's function $G_0(\omega, \boldsymbol{z}|\boldsymbol{z}')$ depends on the shape of the volume V and on the kind of the boundary condition on its surface. In the free-field, i. e. $V = \mathbb{R}^3$ the Green's function for all kinds of boundary conditions is given by [14]

$$G_0^{\mathrm{f}}(\omega, \boldsymbol{z}|\boldsymbol{z}') = \frac{1}{4\pi}\, \frac{e^{-j\frac{\omega}{c}\|\boldsymbol{z} - \boldsymbol{z}'\|}}{\|\boldsymbol{z} - \boldsymbol{z}'\|}\,. \tag{13.18}$$

It describes a spherical wave and is also called the free-field Green's function. The denominator accounts for the decay of the amplitude over distance and the exponential term accounts for the time delay of the propagating spherical wave.

Line Source

A line source consists of a superposition of equal point sources along a line. When the line is oriented in parallel to the z-axis then all point sources with the same xy-coordinates have equal source strength $Q_0(\omega, \boldsymbol{z})$. Consequently, $Q_0(\omega, \boldsymbol{z})$ does not depend on z and the integration in Eq. 13.17 degenerates to an integration in the xy-plane

$$\begin{aligned} Q_0(\omega, \boldsymbol{z}) &= \iiint\limits_V Q_0(\omega, \boldsymbol{z}')\, \delta_{3\mathrm{D}}(\boldsymbol{z} - \boldsymbol{z}')\, d\boldsymbol{z}' \\ &= \iint\limits_L Q_1(\omega, \boldsymbol{x}')\, \delta_{2\mathrm{D}}(\boldsymbol{x} - \boldsymbol{x}') \underbrace{\int\limits_{-\infty}^{\infty} \delta(z - z')\, dz'}_{=1}\, d\boldsymbol{x}' \\ &= Q_1(\omega, \boldsymbol{x})\,, \end{aligned} \tag{13.19}$$

where

$$\delta_{2\mathrm{D}}(\boldsymbol{x}) = \delta(x)\,\delta(y) \tag{13.20}$$

denotes a 2D Dirac-impulse in Cartesian coordinates and L a horizontal cut through the volume V. This result may be interpreted in two ways:

- As before, $Q_0(\omega, \boldsymbol{z})$ describes a collection of point sources (index zero). The three components of $\boldsymbol{z}$ denote the location of each point source in 3D space. However, the source strength is constant in z-direction and therefore the result does not depend on the z-coordinate.
- $Q_1(\omega, \boldsymbol{x})$ describes a collection of line sources parallel to the z-axis. The index one denotes the one-dimensional character of the line sources. The two components of $\boldsymbol{x}$ denote the coordinates of the root points of each line in the xy-plane.

Note that $Q_0(\omega, \boldsymbol{z})$ is a function of three spatial variables (x, y, z) which denote the location of a zero-dimensional entity (a point source) in 3D space. On the other hand, $Q_1(\omega, \boldsymbol{x})$ is a function of two variables (x, y) which denote the location of a one-dimensional entity (a line source parallel to the z-axis). So both $Q_0(\omega, \boldsymbol{z})$ and $Q_1(\omega, \boldsymbol{x})$ describe a 3D sound field with a special structure, i.e. without dependence on the z-coordinate.

The sound field caused by a collection of line sources $Q_1(\omega, \boldsymbol{x})$ can be obtained from Eq.13.17 when $Q_0(\omega, \boldsymbol{z})$ does not depend on z. Then the integration with respect to z' is only performed for the Green's function $G_0(\omega, \boldsymbol{z}|\boldsymbol{z}')$ and yields the Green's function $G_1(\omega, \boldsymbol{x}|\boldsymbol{x}')$ of a line source in parallel to the z-axis

$$G_1(\omega, \boldsymbol{x}|\boldsymbol{x}') = \int_{-\infty}^{\infty} G_0(\omega, \boldsymbol{x}|\boldsymbol{z}')\,dz' \,. \tag{13.21}$$

The resulting sound field is also constant in z-direction and is described by a function $P_1(\omega, \boldsymbol{x})$ depending only on x and y

$$P_1(\omega, \boldsymbol{x}) = \iint_L G_1(\omega, \boldsymbol{x}|\boldsymbol{x}')Q_1(\omega, \boldsymbol{x}')d\boldsymbol{x}' \,. \tag{13.22}$$

The interpretation of $Q_0(\omega, \boldsymbol{z})$ and $Q_1(\omega, \boldsymbol{x})$ in Eq. 13.19 applies in a similar fashion also to $P_0(\omega, \boldsymbol{z})$ and $P_1(\omega, \boldsymbol{x})$.

Evaluating the integral in Eq. 13.21 for the integrand from Eq. 13.18 gives [9, 3.876]

$$G_1^{\mathrm{f}}(\omega, \boldsymbol{x}|\boldsymbol{x}') = -\frac{j}{4}\, H_0^{(2)}\Big(\frac{\omega}{c}\,\rho\Big) \,. \tag{13.23}$$

where $H_0^{(2)}(\frac{\omega}{c}\,\rho)$ is the Hankel function of the second kind and order zero. Due to the circular symmetry, $G_1^{\mathrm{f}}(\omega, \boldsymbol{x}|\boldsymbol{x}')$ depends only on the distance ρ between the listener position $\boldsymbol{x}$ and the line source at $\boldsymbol{x}'$. It is given by (see Fig. 13.2)

$$\rho = \|\boldsymbol{x} - \boldsymbol{x}'\| = \sqrt{(x - x')^2 + (y - y')^2} \,. \tag{13.24}$$

Thus the notation for the Green's function of the line source may be shortened to

$$G_1^{\mathrm{f}}(\omega, \boldsymbol{x}|\boldsymbol{x}') = \tilde{G}_1^{f}(\omega, \rho) = -\frac{j}{4} H_0^{(2)}\left(\frac{\omega}{c}\,\rho\right) . \tag{13.25}$$

In this notation, the Hankel function $H_0^{(2)}$ is given by [9]

$$H_0^{(2)}\left(\frac{\omega}{c}\rho\right) = J_0\left(\frac{\omega}{c}\rho\right) - jN_0\left(\frac{\omega}{c}\rho\right) , \tag{13.26}$$

where $J_0(\frac{\omega}{c}\rho)$ and $N_0(\frac{\omega}{c}\rho)$ are the Bessel and Neumann functions of the first kind and order zero.

13.2.2.3 Relation Between the Green's Functions for Line and Point Sources for the Free Field Case

Now the relation between a line source parallel to the z-axis and a point source at the root point of the line source is investigated for the free-field case. The orientation of the line source and the position of the point source are shown in Fig. 13.2. The effect of both sources on the sound field in the xy-plane is now compared. The effect of the line source is described by $\tilde{G}_1^{\mathrm{f}}(\omega, \rho)$ introduced in Eq. 13.25. The effect of the point source is described by its Green's function (Eq. 13.18) for $z = 0$ and $z' = 0$, i.e. by

$$G_0^{\mathrm{f}}(\omega, \boldsymbol{z}|\boldsymbol{z}')\Big|_{\substack{z\,=\,0\\ z'\,=\,0}} = \tilde{G}_0^{\mathrm{f}}(\omega, \rho) = \frac{1}{4\pi\,\rho}\, e^{-j\left(\frac{\omega}{c}\,\rho\right)} . \tag{13.27}$$

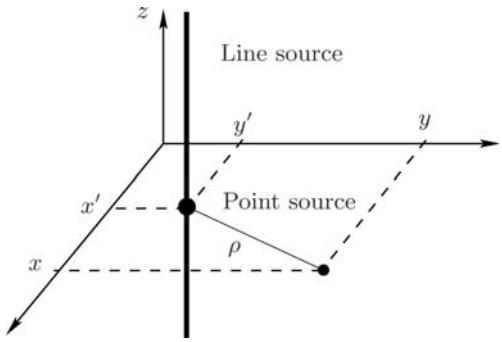

Fig. 13.2. Line source parallel to the z-axis and point source at the root point of the line source in the xy-plane.

The relation between the sound field of a point source in the xy-plane $G_0^{\mathrm{f}}(\omega, \rho)$ and a line source parallel to the z-axis $G_1^{\mathrm{f}}(\omega, \rho)$ is established by an approximation. This approximation can be derived in two different ways, i.e.

through the *method of stationary phase* [26] for the integral in Eq. 13.21 and by the *far-field approximation* [1] for the Green's function $G_l^{\mathrm{f}}(\omega, \rho)$.

The method of stationary phase allows to express certain integrals by the value of their integrand at a fixed argument, the so-called stationary phase point zs through

$$\int_{-\infty}^{\infty} f(\zeta)\, e^{j\phi(\zeta)} d\zeta \approx \sqrt{\frac{2\pi j}{\phi''(z_{\mathrm{s}})}}\; f(z_{\mathrm{s}})\; e^{j\phi(z_{\mathrm{s}})} \tag{13.28}$$

where $\phi''(\zeta)$ denotes the second derivative of $\phi(\zeta)$. This approximation holds for $\phi(\zeta) \gg 1$. The stationary phase point is found by setting the first derivative $\phi'(\zeta)$ of $\phi(\zeta)$ to zero, i.e. $\phi'(z_{\mathrm{s}}) = 0$.

Applying the method of stationary phase to $G_0^{\mathrm{f}}(\omega, \boldsymbol{z}|\boldsymbol{z}')$ with $z = 0$, $z' = \zeta$, and

$$\phi_\rho(\zeta) = -\frac{\omega}{c}\sqrt{\rho^2 + \zeta^2}\,, \qquad f_\rho(\zeta) = \frac{1}{4\pi\sqrt{\rho^2 + \zeta^2}} \tag{13.29}$$

leads to $z_{\mathrm{s}} = 0$ and

$$\tilde{G}_1^{\mathrm{f}}(\omega, \rho) = \int_{\infty}^{\infty} f_\rho(\zeta)\, e^{j\phi_\rho(\zeta)}\, d\zeta \approx \frac{1}{\sqrt{j8\pi\left(\frac{\omega}{c}\,\rho\right)}}\; e^{-j\left(\frac{\omega}{c}\,\rho\right)}\,. \tag{13.30}$$

The same approximation can also be obtained from the asymptotic expansion of the Hankel function for large $|\rho|$ [1]

$$H_0^{(2)}\left(\frac{\omega}{c}\,\rho\right) \approx \sqrt{\frac{2}{\pi\left(\frac{\omega}{c}\,\rho\right)}}\; e^{-j\left(\left(\frac{\omega}{c}\,\rho\right) - \frac{\pi}{4}\right)}\,. \tag{13.31}$$

In acoustics, this expansion is called the far-field approximation of the Hankel function.

Comparing Eqs. 13.25 and 13.30 shows that the effect of a line source on the sound field in the xy-plane may be approximated by the effect of a point source. In particular, $G_1^{\mathrm{f}}(\omega, \rho)$ may be approximated by

$$\tilde{G}_1^{\mathrm{f}}(\omega, \rho) = H(\omega)\; A(\rho)\; \tilde{G}_0^{\mathrm{f}}(\omega, \rho)\,, \tag{13.32}$$

where

$$H(\omega) = \sqrt{\frac{c}{j\omega}} \tag{13.33}$$

causes a spectral shaping and

$$A(\rho) = \sqrt{2\pi\,\rho} \tag{13.34}$$

causes an amplitude modification of $\tilde{G}_0^{\mathrm{f}}(\omega, \rho)$.

The derivation from Eq. 13.23 to Eq. 13.34 on the relation between line sources and point sources may be summarized as follows:

- The evaluation of the integral in Eq. 13.21 with the stationary phase method leads to the far-field approximation of the Green's function of a line source.
- The effect of a line source on the xy-plane can be approximated by a point source at the root point of the line source. The sound field of the point source has to be corrected by spectral shaping and an amplitude modification. This approximation is valid in the far-field of the line source.

13.2.3 Kirchhoff-Helmholtz Integral

The Kirchhoff-Helmholtz integral is the key element of the wave field synthesis principle. It provides the relation between the sound field inside a volume of arbitrary shape and on the enclosing boundary. The Kirchhoff-Helmholtz-Integral is presented first for a general 3D volume and then specialized to a 3D prism.

13.2.3.1 Kirchhoff-Helmholtz Integral for a General 3D Volume

The *Kirchhoff-Helmholtz integral* or *Helmholtz integral equation* expresses the values $P_0(\omega, \boldsymbol{z})$ inside a volume V by an integral on the surface ∂V [14,16,26]

$$-\oiint_{\partial V} \left(G_0(\omega, \boldsymbol{z}|\boldsymbol{z}') \, \frac{\partial}{\partial \boldsymbol{n}} P_0(\omega, \boldsymbol{z}') - P_0(\omega, \boldsymbol{z}') \, \frac{\partial}{\partial \boldsymbol{n}} G_0(\omega, \boldsymbol{z}|\boldsymbol{z}') \right) d\boldsymbol{z}' = \\ = \begin{cases} P_0(\omega, \boldsymbol{z}) \,, & \boldsymbol{z} \in V \\ 0 \,, & \boldsymbol{z} \notin V \end{cases} . \quad (13.35)$$

$G_0(\omega, \boldsymbol{z}|\boldsymbol{z}')$ is a Green's function which satisfies suitable boundary conditions on ∂V.

The Kirchhoff-Helmholtz integral states that at any point within the source-free region V the sound pressure $P_0(\omega, \mathbf{z})$ can be calculated if both the sound pressure $P_0(\omega, \boldsymbol{z}')$ and its directional gradient $\frac{\partial}{\partial \boldsymbol{n}} P_0(\omega, \boldsymbol{z}')$ are known on the boundary ∂V enclosing the volume. The boundary ∂V does not necessary have to be a real physical existing surface. The Kirchhoff-Helmholtz integral is typically used in three areas: (1) the calculation of a sound field emitted by a vibrating surface into a region, (2) the calculation of a sound field inside a finite region produced by a source outside the volume from measurements on the surface and (3) the acoustic control over the sound field within a volume. The third application area leads to sound reproduction according to the principle of wave field synthesis [22, 24].

13.2.3.2 Kirchhoff-Helmholtz Integral for a Prism

The Kirchhoff-Helmholtz integral is now specialized to sound fields which do not depend on the z-coordinate. The shape of the volume for the integration in Eq. 13.35 turns into a prism oriented in parallel to the z-axis (see

Fig. 13.3). This rather special spatial arrangement allows the transition to a 2D description of the Kirchhoff-Helmholtz integral. The stages of this transition are shown for the first term in Eq. 13.35. The presented procedure applies equally to the second term.

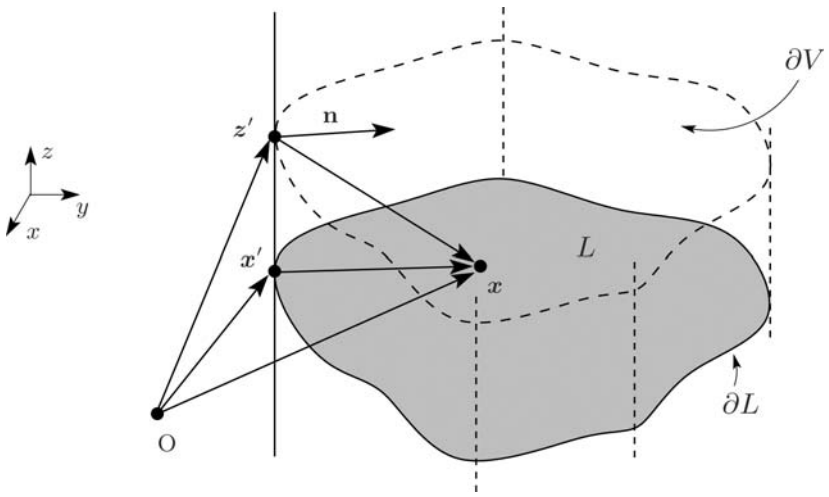

Fig. 13.3. Illustration of a sound field with does not depend on the z-coordinate.

Since the sound field is assumed to be independent of z, $P_0(\omega, \boldsymbol{z})$ depends only on x and y. Furthermore, any vector normal to the surface ∂V has no component in the z-direction and also the normal derivative of $P_0(\omega, \boldsymbol{z})$ is independent of z. Thus the surface integration with respect to $\boldsymbol{z}'$ in Eq. 13.35 can be split into a contour integration with respect to $\boldsymbol{x}'$ and an integration with respect to z'. The contour ∂L is defined by the intersection of the prism with the xy-plane. This procedure turns the first term of Eq. 13.35 into

$$\begin{aligned}
&\iint\limits_{\partial V} G_0(\omega, \boldsymbol{z}|\boldsymbol{z}') \, \frac{\partial}{\partial \boldsymbol{n}} P_0(\omega, \boldsymbol{z}') \, d\boldsymbol{z}' \\
&= \oint\limits_{\partial L} \int\limits_{-\infty}^{\infty} G_0(\omega, \boldsymbol{z}|\boldsymbol{z}') \, \frac{\partial}{\partial \boldsymbol{n}} P_0(\omega, \boldsymbol{z}') \, dz' \, d\boldsymbol{x}' \\
&= \oint\limits_{\partial L} \left[\int\limits_{-\infty}^{\infty} G_0(\omega, \boldsymbol{z}|\boldsymbol{z}') \, dz' \right] \, \frac{\partial}{\partial \boldsymbol{n}} P_0(\omega, \boldsymbol{z}') \, d\boldsymbol{x}' \, . \qquad (13.36)
\end{aligned}$$

With Eq. 13.21 follows a 2D version of the Kirchhoff-Helmholtz-Integral

$$P_1(\omega, \boldsymbol{z}) = -\oint_{\partial L} \left(G_1(\omega, \boldsymbol{x}|\boldsymbol{x}') \frac{\partial}{\partial \boldsymbol{n}} P_1(\omega, \boldsymbol{x}') - P_1(\omega, \boldsymbol{x}') \frac{\partial}{\partial \boldsymbol{n}} G_1(\omega, \boldsymbol{x}|\boldsymbol{x}') \right) d\boldsymbol{x}'. \tag{13.37}$$

13.3 Wave Field Synthesis

13.3.1 Introduction

In the following the sound reproduction scenario depicted in Fig. 13.4 will be considered. The wave field emitted by an arbitrary virtual source $Q_0(\omega, \boldsymbol{z})$

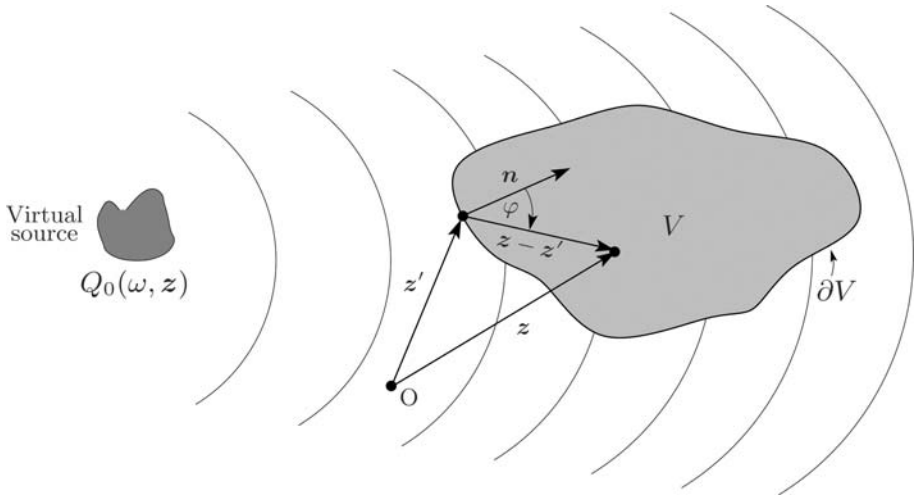

Fig. 13.4. Reproduction of the spatial wave field emitted by the virtual source inside the bounded region V and parameters used for the Kirchhoff-Helmholtz integral (Eq. 13.35).

should be reproduced in the bounded region V. This region will be termed as *listening region* in the following, since the listeners reside there. The virtual source $Q_0(\omega, \boldsymbol{z})$ may not have contributions in V. The limitation to one virtual source poses no constraints on the wave field to be reproduced, since this source may have arbitrary shape and frequency characteristics. Additionally, multiple sources can be reproduced by the principle of superposition.

The basic principle of sound reproduction can be illustrated with the principle of Huygens [14]. Huygens stated that any point of a propagating wave front at any time-instant conforms to the envelope of spherical waves emanating from every point on the wavefront at the prior instant. This principle can be used to synthesize acoustic wavefronts of arbitrary shape. Of course, it is not very practical to position the acoustic sources on the wavefronts

for synthesis. By placing the loudspeakers on an arbitrary fixed curve and by weighting and delaying the driving signals, an acoustic wavefront can be synthesized with a loudspeaker array. Fig. 13.5 illustrates this principle. The

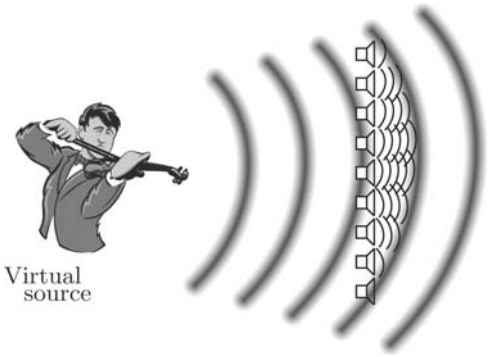

Fig. 13.5. Application of Huygens principle to perform sound reproduction.

mathematical foundation of this more illustrative description to sound reproduction is given by the Kirchhoff-Helmholtz integral. It was introduced in Sec. 13.2.3 and will be utilized in the following to derive a generic theory of sound reproduction systems.

13.3.2 Kirchhoff-Helmholtz Integral based Sound Reproduction

The Kirchhoff-Helmholtz integral (Eq. 13.35) comprises a number of different problems as already addressed in Sec. 13.2.3.1. Each of these issues is characterized by its specific type of boundary conditions and thus by the corresponding Green's function.

For the sound reproduction scenario according to Fig. 13.4 the Green's function $G_0(\omega, \boldsymbol{z}|\boldsymbol{z}')$ and its directional gradient can be understood as the field emitted by sources placed on ∂V. These sources will be termed as *secondary sources* in the following. The strength of these sources is determined by the pressure $P_0(\omega, \boldsymbol{z}')$ and the directional pressure gradient $\frac{\partial}{\partial \boldsymbol{n}} P_0(\omega, \boldsymbol{z}')$ of the virtual source field $Q_0(\omega, \boldsymbol{x}')$ on ∂V.

Thus, this specialized Kirchhoff-Helmholtz integral can be interpreted as follows: If appropriately chosen secondary sources are driven by the sound pressure and the directional pressure gradient of the wave field emitted by the virtual source $Q_0(\omega, \boldsymbol{x}')$ on the boundary ∂V, then the wave field within the region V is equivalent to the wave field which would have been produced by the virtual source inside V. Thus, the theoretical basis of sound reproduction is described by the Kirchhoff-Helmholtz integral (Eq. 13.35).

The three-dimensional free-field Green's function is given by Eq. 13.18. In the context of sound reproduction it can be interpreted as the field of

a monopole point source distribution on the surface ∂V. The Kirchhoff-Helmholtz integral (Eq. 13.35) also involves the directional gradient of the Green's function. The directional gradient of the three-dimensional free-field Green's function can be interpreted as the field of a dipole source whose main axis lies in direction of the normal vector $\boldsymbol{n}$. Thus, the Kirchhoff-Helmholtz integral states in this case, that the acoustic pressure inside the volume V can be controlled by a monopole and a dipole point source distribution on the surface ∂V enclosing the volume V.

This interpretation of the Kirchhoff-Helmholtz integral sketches a first draft of a technical system for spatial sound reproduction. In rough terms, such a system would consist of technical approximations of acoustical monopoles and dipoles by appropriate loudspeakers. These loudspeakers cover the surface of a suitably chosen volume around the possible listener positions. They are excited by appropriate driving functions to reproduce the desired sound field inside the volume.

However, there remain a number of fundamental questions to be resolved on the way to a technical realization. Four major areas can be identified. They are listed below and are discussed in detail in the following sections.

Monopole and Dipole Sources.

Technical approximations of acoustical monopoles and dipoles consist of loudspeakers with different types of enclosures. A restriction to only one type of sources would be of advantage for a technical realization. For example the use of monopole sources only facilitates a technical solution with small loudspeakers in closed cabinets.

Reduction to Two Spatial Dimensions.

The volume V certainly has to be large enough to enclose at least a small audience or to give a single listener room to move within the sound field. Covering the whole surface with suitable sound sources appears to be a technological and economical challenge. Furthermore, it may not be required to reproduce the sound field within the entire volume. A correct reproduction in a horizontal plane at the level of the listeners' ears may be sufficient. Such a simplification requires to reduce the 3D problem to two spatial dimensions.

Spatial Sampling.

The Kirchhoff-Helmholtz integral prescribes a continuous source distribution over the surface ∂V. However, an approximation of sound sources by loudspeakers results in a spatially discrete source distribution. The resulting discretization effects may be described in terms of spatial sampling.

Driving Signals.

Once the source distribution is approximated by a sufficiently dense grid of loudspeakers, their driving signals have to be generated by signal processing hardware and digital-to-analog converters.

13.3.3 Monopole and Dipole Sources

The use of monopole and dipole sources in Eq. 13.35 allows a very precise reproduction of the desired wave field: It is recreated as $P_0(\omega, z)$ for all positions inside of V and it is zero outside. Such a restriction is usually not required for spatial sound reproduction. As long as the reproduction is correct inside of V, almost arbitrary sound fields outside may be tolerated, as long as their reproduction volume is moderate. This situation suggests the following trade-off: Use one type of sound sources only and tolerate some sound pressure outside of V.

To realize this trade-off, a Green's function $G_0(\omega, \boldsymbol{z}|\boldsymbol{z'})$ is constructed which satisfies boundary conditions of the first or second kind on the surface ∂V. Since it is desirable to drop the dipoles and to keep the monopole sources, the Green's function of a point source $G_0^{\mathrm{f}}(\omega, \boldsymbol{z}|\boldsymbol{z'})$ according to Eq. 13.18 is chosen as the basic building block. Then for each position z' on the boundary, the Green's function $G_0^{\mathrm{f}}(\omega, \boldsymbol{z}|\boldsymbol{z'})$ for a position z inside of V and the Green's function $G_0^{\mathrm{f}}(\omega, \bar{\boldsymbol{z}}(\boldsymbol{z})|\boldsymbol{z'})$ for a position $\bar{\boldsymbol{z}}(\boldsymbol{z})$ outside of V are superposed

$$G_0(\omega, \boldsymbol{z}|\boldsymbol{z'}) = G_0^{\mathrm{f}}(\omega, \boldsymbol{z}|\boldsymbol{z'}) + G_0^{\mathrm{f}}(\omega, \bar{\boldsymbol{z}}(\boldsymbol{z})|\boldsymbol{z'}) \; . \tag{13.38}$$

The position $\bar{\boldsymbol{z}}(\boldsymbol{z})$ is chosen as the mirror image of $\boldsymbol{z}$ with respect to the tangent plane in $\boldsymbol{z}'$ on the surface ∂V (see Fig. 13.6). The tangent plane is characterized by the unit vector $\boldsymbol{n}$. The notation $\bar{\boldsymbol{z}}(\boldsymbol{z})$ indicates that $\bar{\boldsymbol{z}}$ depends on $\boldsymbol{z}$.

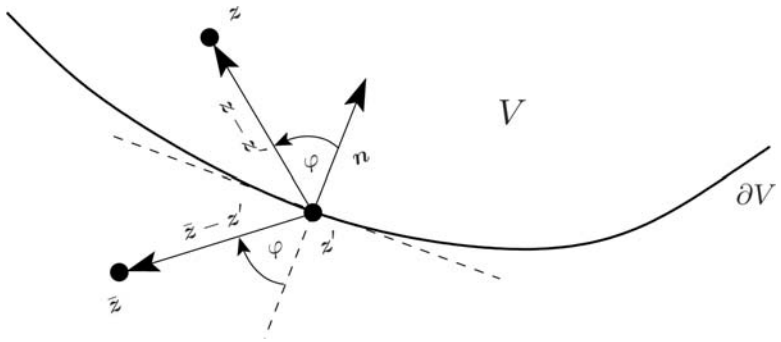

Fig. 13.6. Illustration of the geometry used for the derivation of the modified Green's function for a sound reproduction system using monopole secondary sources only.

From the symmetry of the mirror images follows

$$\left\|\boldsymbol{z} - \boldsymbol{z'}\right\| = \left\|\bar{\boldsymbol{z}}(\boldsymbol{z}) - \boldsymbol{z'}\right\| = \rho_z \; , \tag{13.39}$$

and thus the functional dependence of $G_0^{\mathrm{f}}(\omega, \boldsymbol{z}|\boldsymbol{z'})$ and $G_0^{\mathrm{f}}(\omega, \bar{\boldsymbol{z}}(\boldsymbol{z})|\boldsymbol{z'})$ on $\boldsymbol{z}$ and $\boldsymbol{z'}$ is identical

$$G_0^{\mathrm{f}}(\omega, \boldsymbol{z}|\boldsymbol{z'}) = G_0^{\mathrm{f}}(\omega, \bar{\boldsymbol{z}}(\boldsymbol{z})|\boldsymbol{z'}) \; . \tag{13.40}$$

However, $G_0^{\mathrm{f}}(\omega, \boldsymbol{z}|\boldsymbol{z'})$ and $G_0^{\mathrm{f}}(\omega, \bar{\boldsymbol{z}}(\boldsymbol{z})|\boldsymbol{z'})$ have to be carefully distinguished as Green's functions for positions inside of V and outside of V, respectively. This difference becomes apparent for the gradients

$$\begin{aligned} \nabla G_0^{\mathrm{f}}(\omega, \boldsymbol{z}|\boldsymbol{z'}) &= -\frac{1 + jk\rho_z}{\rho_z} \; G_0^{\mathrm{f}}(\omega, \boldsymbol{z}|\boldsymbol{z'}) \; \boldsymbol{n_z} \\ \nabla G_0^{\mathrm{f}}(\omega, \bar{\boldsymbol{z}}|\boldsymbol{z'}) &= -\frac{1 + jk\rho_z}{\rho_z} \; G_0^{\mathrm{f}}(\omega, \bar{\boldsymbol{z}}|\boldsymbol{z'}) \; \boldsymbol{n_{\bar{z}}} \; , \end{aligned} \tag{13.41}$$

with the unit vectors

$$\boldsymbol{n_z} = \frac{\boldsymbol{z} - \boldsymbol{z'}}{\left\|\boldsymbol{z} - \boldsymbol{z'}\right\|} \; , \qquad \boldsymbol{n_{\bar{z}}} = \frac{\bar{\boldsymbol{z}} - \boldsymbol{z'}}{\left\|\bar{\boldsymbol{z}} - \boldsymbol{z'}\right\|} \; . \tag{13.42}$$

The derivative with respect to $\boldsymbol{n}$ is given by

$$\frac{\partial}{\partial \boldsymbol{n}} G_0^{\mathrm{f}}(\omega, \boldsymbol{z}|\boldsymbol{z'}) = \left\langle \nabla G_0^{\mathrm{f}}(\omega, \boldsymbol{z}|\boldsymbol{z'}), \boldsymbol{n} \right\rangle = -\frac{1 + jk\rho_z}{\rho_z} \; G_0^{\mathrm{f}}(\omega, \boldsymbol{z}|\boldsymbol{z'}) \left\langle \boldsymbol{n_z}, \boldsymbol{n} \right\rangle \tag{13.43}$$

and similarly for the derivative of $G_0^{\mathrm{f}}(\omega, \bar{\boldsymbol{z}}|\boldsymbol{z'})$. With Eq. 13.40 and (see Fig. 13.6)

$$\left\langle \boldsymbol{n_z}, \boldsymbol{n} \right\rangle + \left\langle \boldsymbol{n_{\bar{z}}}, \boldsymbol{n} \right\rangle = 0 \tag{13.44}$$

follows

$$\frac{\partial}{\partial \boldsymbol{n}} G_0(\omega, \boldsymbol{z}|\boldsymbol{z'}) = \frac{\partial}{\partial \boldsymbol{n}} G_0^{\mathrm{f}}(\omega, \boldsymbol{z}|\boldsymbol{z'}) + \frac{\partial}{\partial \boldsymbol{n}} G_0^{\mathrm{f}}(\omega, \bar{\boldsymbol{z}}|\boldsymbol{z'}) = 0 \, , \quad \boldsymbol{z'} \in \partial V \, . \tag{13.45}$$

In summary, the Green's function $G_0(\omega, \boldsymbol{z}|\boldsymbol{z'})$ according to Eq. 13.38 induces a sound field not only inside of V but also on the outside. On the other hand, the normal derivative of $G_0(\omega, \boldsymbol{z}|\boldsymbol{z'})$ is zero for all positions $\boldsymbol{z'}$ on the boundary ∂V. Thus inserting $G_0(\omega, \boldsymbol{z}|\boldsymbol{z'})$ as Green's function into the Kirchhoff-Helmholtz integral (Eq. 13.35) leads to

$$P_0(\omega, \boldsymbol{z}) = -\iint\limits_{\partial V} G_0(\omega, \boldsymbol{z}|\boldsymbol{z'}) \; \frac{\partial}{\partial \boldsymbol{n}} P_0(\omega, \boldsymbol{z'}) \, d\boldsymbol{z'} \, , \qquad \boldsymbol{z} \in V \, . \tag{13.46}$$

Since $G_0(\omega, \boldsymbol{z}|\boldsymbol{z'})$ is equal to $G_0^{\mathrm{f}}(\omega, \boldsymbol{z}|\boldsymbol{z'})$ for sources inside of V, the result of Eq. 13.46 is equal to the desired wave field $P_0(\omega, \boldsymbol{z})$ inside of V. Outside of V the wave field consists of a mirrored version of the wave field inside of V. An example is shown in Fig. 13.8. The result (Eq. 13.46) is also known as the type-I Raleigh integral [22].

It states that the sound field inside of a volume V may be reproduced by a distribution of point sources if a mirrored version of this sound field is tolerated outside of V. If only the monopole properties of this Green's function are or interest, then Eq. 13.21 may be expressed with Eq. 13.40 as

$$G_0(\omega, \boldsymbol{z}|\boldsymbol{z'}) = 2\, G_0^{\mathrm{f}}(\omega, \boldsymbol{z}|\boldsymbol{z'}) \;, \tag{13.47}$$

i.e. the boundary sources as free-field point sources with double strength. The factor of two follows from the fact that these point sources describe the contribution inside and outside of V in equal terms.

These considerations are summarized by Eq. 13.48 below. The sound field inside $P_0(\omega, \boldsymbol{z})$ of a volume V can be generated by a distribution of monopole sources on the surface ∂V. The field outside of V will not vanish as in Eq. 13.35, since no more dipole sources are involved. Furthermore, the construction of the Green's function according to Eq. 13.38 induces boundary conditions of the second kind (Neumann) on the surface ∂V

$$P_0(\omega, \boldsymbol{z}) = -\iint\limits_{\partial V} 2\, G_0^{\mathrm{f}}(\omega, \boldsymbol{z}|\boldsymbol{z'})\, \frac{\partial}{\partial \boldsymbol{n}} P_0(\omega, \boldsymbol{z'})\, d\boldsymbol{z'} \;, \qquad \boldsymbol{z} \in V \;. \tag{13.48}$$

The effects of these boundary conditions are considered for the determination of the driving signals in Sec. 13.3.6.

13.3.4 Reduction to Two Spatial Dimensions

The requirement of creating a distribution of sources on a whole surface around a listening space may be impractical for many sound reproduction systems. This section shows how to reduce the source distribution from a surface around the listeners to a closed curve in a horizontal plane preferably in the height of the listeners' ears. For convenience this height is denoted by $z = 0$.

The mathematical tools for the reduction of the source distribution have already been presented by considering the Kirchhoff-Helmholtz integral for a prism in Sec. 13.2.3.2 and the relations between line and point sources in Sec. 13.2.2.3. These considerations are now applied in two steps to the representation of a spatial sound field in Eq. 13.48.

The first step is the conversion of the general surface ∂V to a prism. Performing the mathematical operations in Eq. 13.36 on Eq. 13.48 results in a representation of the 3D sound field in a prism which is independent of z (compare Eq. 13.37)

$$P_1(\omega, \boldsymbol{x}) = -\oint\limits_{\partial L} 2\, G_1^{\mathrm{f}}(\omega, (\boldsymbol{x}|\boldsymbol{x'})\, \frac{\partial}{\partial \boldsymbol{n}} P_1(\omega, \boldsymbol{x'})\, d\boldsymbol{x'} \;, \qquad \boldsymbol{x} \in L \;. \tag{13.49}$$

This relation describes a distribution of line sources parallel to the z-axis. However, a technical realization would not be easy to implement.

To arrive at a model for a practical solution, a second step replaces the line sources by point sources according to Sec. 13.2.2.3. With Eq. 13.32 follows from Eq. 13.49

$$P_1(\omega, \boldsymbol{x}) = -\oint_{\partial L} G_0^{\mathrm{f}}(\omega, \boldsymbol{x}|\boldsymbol{x}')\, D(\omega, \boldsymbol{x}|\boldsymbol{x}')\, d\boldsymbol{x}' \,, \qquad \boldsymbol{x} \in L \,, \tag{13.50}$$

with

$$D(\omega, \boldsymbol{x}|\boldsymbol{x}') = 2A\big(\|\boldsymbol{x} - \boldsymbol{x}'\|\big)\, H(\omega)\, \frac{\partial}{\partial \boldsymbol{n}} P_1(\omega, \boldsymbol{x}') \,. \tag{13.51}$$

To show the dependence on $\boldsymbol{x}$ and $\boldsymbol{x}'$, ρ in Eq. 13.32 has been expanded by Eq. 13.24.

In Eq. 13.50, $G_0^{\mathrm{f}}(\omega, \boldsymbol{x}|\boldsymbol{x}')$ denotes the Green's function of the monopole sources on the contour ∂L in the xy-plane. It describes the wave propagation in 3D space, however, the receiver locations $\boldsymbol{x}$ (the listeners' ears) are assumed to reside in the xy-plane as well. $D(\omega, \boldsymbol{x}|\boldsymbol{x}')$ denotes the source signal of the monopoles.

13.3.5 Spatial Sampling

The previous sections showed how the rather general statement of the Kirchhoff-Helmholtz integral can be narrowed down to a model for a spatial reproduction system. A hypothetical distribution of monopole and dipole sources on a 2D surface around the listener has been replaced by a distribution of monopoles on a 1D contour in a horizontal plane in the height of the listeners' ears.

For a technical solution, this spatially continuous source distribution has to be replaced by an arrangement of a finite number of loudspeakers with a monopole-like source directivity. The resulting wave field is given by a modification of Eq. 13.50, where the integral is substituted by a sum over the discrete loudspeaker positions $\boldsymbol{x}'_n$

$$P_1(\omega, \boldsymbol{x}) \approx -\sum_n G_0^{\mathrm{f}}(\omega, \boldsymbol{x}|\boldsymbol{x}'_n)\, D(\omega, \boldsymbol{x}|\boldsymbol{x}'_n)\, \Delta x'_n \,. \tag{13.52}$$

$\Delta x'_n$ is the length of the spatial increment $\Delta \boldsymbol{x}'_n$ between the samples. It is not required to be equidistant.

The representation of a continuous function by a finite number of spatially discrete sources is known as spatial sampling in terms of signal theory. Unfortunately, spatial sampling of wave fields is not yet satisfactorily described in the technical literature. Therefore, some general remarks have to suffice at this point.

Sampling of multidimensional functions is well understood, e.g. in image or video processing. However, deriving a suitable loudspeaker spacing from the requirement of the sampling theorem demands to place two loudspeakers per shortest permissible wavelength. For the usual audio range up to 20 kHz, loudspeakers would have to be placed at a distance of less than 1 cm. Such a loudspeaker array is not technically feasible, considering both the size of available loudspeakers as well es their total number.

It appears that there are two factors of influence, which allow to reduce the number of loudspeakers significantly. At first, a wave field is not an arbitrary signal restricted only by an upper bound of its frequency range. Instead, all signals in acoustics are solutions of the wave equation. This special property restricts the frequency domain representations of wave fields significantly [17]. The consequences for sampling of wave fields have been described e.g. in [7].

The second factor is the human perception of spatial aliasing effects. Experience with existing wave field synthesis implementations with loudspeaker spacing between 10 cm and 20 cm suggests that aliasing terms in sound fields are subject to effective masking by other sound components. However, working knowledge in human perception of spatial aliasing seems to be still rather restricted. For some further comments on spatial sampling see e.g. [21]. In short, spatial sampling seems to be a useful approach for spatial reproduction, although the human perception of its effects is largely unexplored.

13.3.6 Driving Signals

It remains to determine the driving signals of the loudspeakers. They follow from an analysis of $D(\omega, \boldsymbol{x}|\boldsymbol{x}')$ according to Eq. 13.51. This analysis has to take the nature of the desired wave field into account. Wave fields may be modeled by arrangements of different types of sources, e.g. monopoles and dipoles, and by plane waves. The determination of the driving signals from a model of the wave field is called *model based rendering*. On the other hand, a wave field can be recorded in a natural environment like a concert hall or a church. Obtaining the driving signals from a recorded wave field is called *data based rendering*.

The determination of the driving signals is shown here for a rather general case of model based rendering, where the desired wave field is given by a decomposition into plane waves according to Eq. 13.11. The discussion focusses on three major points:

1. The correct consideration of the boundary conditions (Eq. 13.45) induced by the choice of the Green's function for the elimination of the dipole sources in Sec. 13.3.3.
2. The determination of the normal derivative in Eq. 13.51.
3. The independence of the driving signals from the listener position.

13.3.6.1 Boundary Conditions

The elimination of the dipole sources in Sec. 13.3.3 was based on the choice of a Green's function with homogeneous boundary conditions of the second kind (Neumann), i.e. a vanishing normal derivative on the boundary (see Eq. 13.45). Boundary conditions of this kind are known to produce reflections on the boundary. At first sight it is not clear, how these reflections should

occur, since the boundary ∂L is only an arbitrary contour for the placement of point sources and not a solid wall.

For a better understanding of the situation, consider Fig. 13.7. It shows a contour ∂L in a plane with two different monopole positions. These positions are spatial samples $\boldsymbol{x}'_n$ of the coordinate $\boldsymbol{x}'$ on ∂L. Since these positions are arbitrary, the indication of the sample number n will be suppressed for ease of notation. Note that the monopole positions are not only characterized by their coordinates $\boldsymbol{x}'$ but also by the normal vector $\boldsymbol{n}$ on the contour ∂L at $\boldsymbol{x}'$ and by the angle γ according to

$$\boldsymbol{n} = \begin{bmatrix} \cos\gamma \\ \sin\gamma \end{bmatrix} . \tag{13.53}$$

The monopoles shall be driven such that they produce a plane wave in the direction $\boldsymbol{n}_\theta$. Obviously the contour ∂L exhibits two different sections separated by circles in Fig. 13.7. Monopoles in the left section emanate waves into the domain L with a component in the direction $\boldsymbol{n}_\theta$ of the plane wave. Producing circular waves, they also radiate a component into the direction opposite to $\boldsymbol{n}_\theta$, but it does not effect the domain L. However a monopole in the right section emanates into L a component opposite to $\boldsymbol{n}_\theta$. The superposition of monopoles and dipoles required by the Kirchhoff-Helmholtz integral creates a directivity which prevents source components in the wrong direction. But with monopoles only, there is no other way than accepting equal sound radiation in all directions.

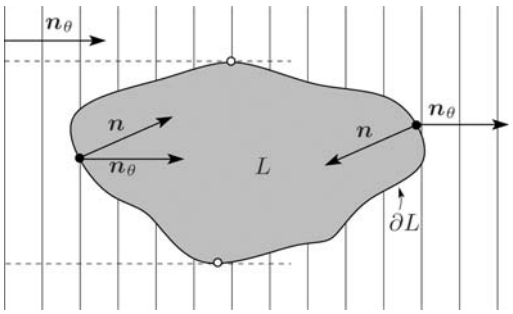

Fig. 13.7. Reproduction of a plane wave by a monopoles on a contour ∂L.

On the other hand, the radiation of the monopoles in the right section of Fig. 13.7 into the domain L equals the reflections that would have been produced by a hard surface at ∂L. Although such a reflecting wall is not physically present, its reflections are produced by the monopoles in the right section. However these components travelling in the direction opposite to $\boldsymbol{n}_\theta$ do not belong to the desired wave field. Since dipoles are no more available to solve the problem in the domain of acoustics, the reflections in the right section have to be counteracted by suitable processing of the driving signals.

A simple but effective way to prevent sound radiation in the wrong direction is to cancel the driving signals of the loudspeakers in the right section. This measure is described by a rectangular window function $v(\boldsymbol{x}', \theta)$ which determines the source activity for each location $\boldsymbol{x}'$ on the contour ∂L and for each possible direction θ of a plane wave. The values of the window function depend on the scalar product $\langle \boldsymbol{n}, \boldsymbol{n}_\theta \rangle$ between the direction $\boldsymbol{n}_\theta$ of plane wave propagation and the normal vector $\boldsymbol{n}$ in each position $\boldsymbol{x}'$ on ∂L. Since $\langle \boldsymbol{n}, \boldsymbol{n}_\theta \rangle = \cos(\theta - \gamma)$, the window function is defined as

$$v(\boldsymbol{x}', \theta) = \begin{cases} 1, & \text{if} \quad \langle \boldsymbol{n}, \boldsymbol{n}_\theta \rangle > 0 \quad \text{or} \quad |\theta - \gamma| < \dfrac{\pi}{2}\,, \\ 0, & \text{else.} \end{cases} \tag{13.54}$$

With this window function, the source signal for the monopoles from Eq. 13.51 can be written as

$$D(\omega, \boldsymbol{x}|\boldsymbol{x}') = 2v(\boldsymbol{x}', \theta)\, A\big(\|\boldsymbol{x} - \boldsymbol{x}'\|\big)\, H(\omega)\, \frac{\partial}{\partial \boldsymbol{n}} P_1(\omega, \boldsymbol{x}')\,. \tag{13.55}$$

As an example, the wave field reproduced by a circular distribution of monopole sources is shown in Fig. 13.8. The radius of the circular region was chosen as $R = 1.50$ m. Two cases where evaluated: (1) the left row shows the results when the window function $v(\boldsymbol{x}', \theta)$ is discarded, (2) the right row shows the results when incorporating the window function.

From the results it can be clearly seen that the window function eliminates the reflections introduced by the Neumann boundary conditions. The wave field is reproduced correctly within the circular distribution of secondary monopole sources. The wave field outside of that region does not vanish, as this would be the case when using both monopole and dipole sources. Instead it is a mirrored version of the plane wave within the circle (see Fig. 13.6).

13.3.6.2 Determination of the Normal Derivative

To calculate the driving signal from Eq. 13.55 requires to express the normal derivative of $P_1(\omega, \boldsymbol{x}')$ by a suitable characterization of the wave field. Here, wave fields with a representation as a plane wave decomposition are considered. Then the normal derivative has to be expressed by the plane wave coefficients (see Sec. 13.2.2.1), i.e. by the wave forms of the individual plane wave components.

First, only a single plane wave is investigated. According to Eq. 13.10 its influence at the loudspeaker position $\boldsymbol{x}'$ is given by

$$P_1(\omega, \boldsymbol{x}') = F(\omega, \theta)\; e^{j\frac{\omega}{c}\langle \boldsymbol{x}', \boldsymbol{n}_\theta \rangle}\,, \tag{13.56}$$

For the gradient $\nabla P_1(\omega, \boldsymbol{x}')$ follows

$$\nabla P_1(\omega, \boldsymbol{x}') = j\frac{\omega}{c}\, P_1(\omega, \boldsymbol{x}')\, \boldsymbol{n}_\theta \tag{13.57}$$

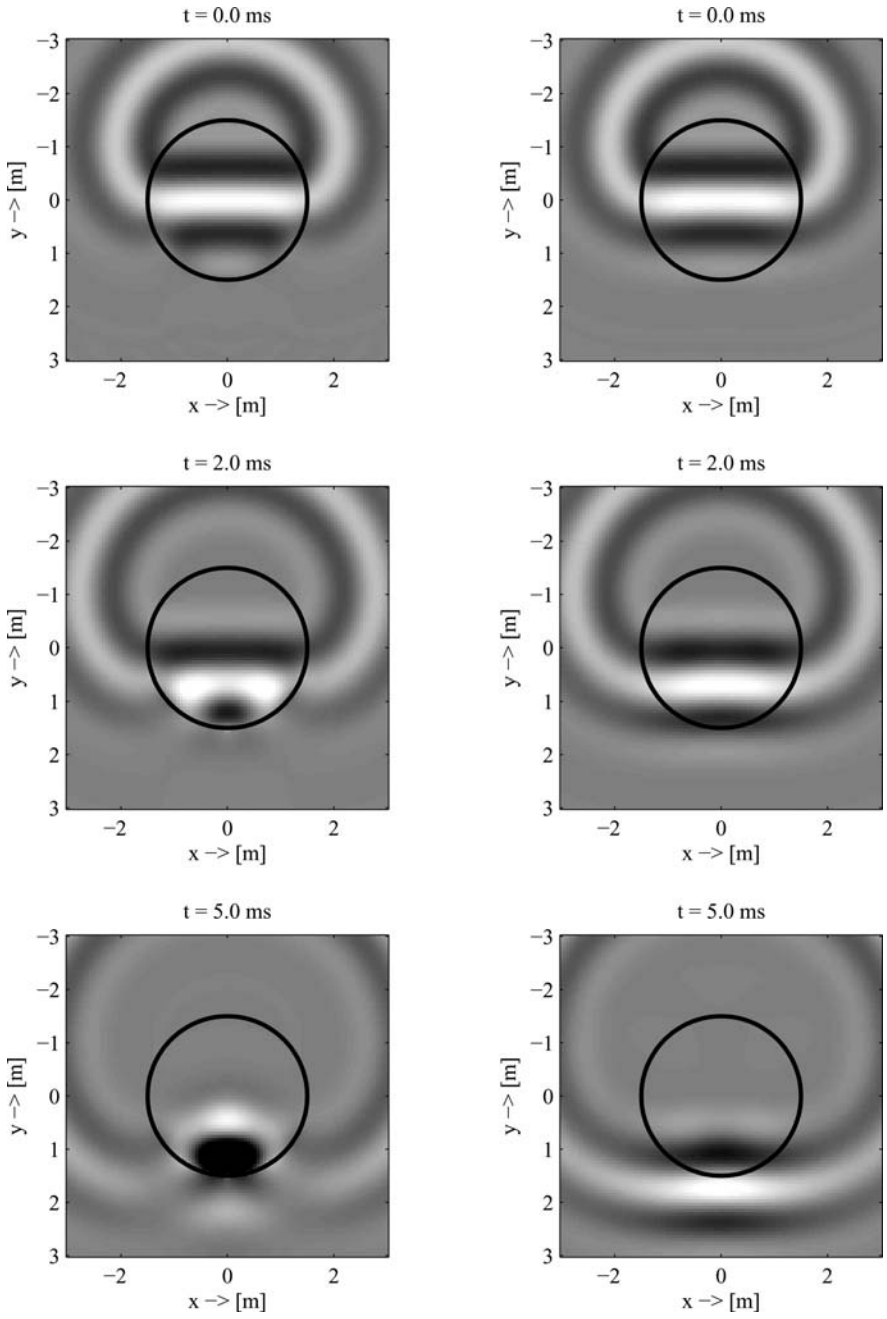

Fig. 13.8. Reproduction of a plane wave with a two-dimensional circular distribution of monopole sources. The left row shows the wave field when discarding the window function $v(\boldsymbol{x}', \theta)$, the right row when taking it into account.

and for the normal derivative

$$\begin{aligned}\frac{\partial}{\partial \boldsymbol{n}} P_1(\omega, \boldsymbol{x}') &= \Big\langle \nabla P_1(\omega, \boldsymbol{x}'), \boldsymbol{n} \Big\rangle \\ &= j\frac{\omega}{c}\, P_1(\omega, \boldsymbol{x}')\, \langle \boldsymbol{n}_\theta, \boldsymbol{n} \rangle \\ &= j\frac{\omega}{c}\, P_1(\omega, \boldsymbol{x}')\, \cos(\theta - \gamma). \end{aligned} \tag{13.58}$$

Inserting the normal derivative (Eq. 13.58) into Eq. 13.55 gives the driving signal $D_\theta(\omega, \boldsymbol{x}|\boldsymbol{x}')$ for a plane wave with the angle of incidence θ. After some manipulations, the result may be written as

$$D_\theta(\omega, \boldsymbol{x}|\boldsymbol{x}') = 2w(\boldsymbol{x}', \theta)\, A\big(\|\boldsymbol{x} - \boldsymbol{x}'\|\big)\, K(\omega)\, e^{j\frac{\omega}{c}\langle \boldsymbol{x}', \boldsymbol{n}_\theta \rangle}\, F(\omega, \theta)\,. \tag{13.59}$$

The various terms of $D_\theta(\omega, \boldsymbol{x}|\boldsymbol{x}')$ are now discussed in detail.

- The window function $w(\boldsymbol{x}', \theta)$ combines the effects of the rectangular window function $v(\boldsymbol{x}', \theta)$ from Eq. 13.54 and the cos-term from the normal derivative in Eq. 13.58

$$w(\boldsymbol{x}', \theta) = \begin{cases} \cos(\theta - \gamma), & \text{if} \quad |\theta - \gamma| < \dfrac{\pi}{2}\,, \\ 0, & \text{else.} \end{cases} \tag{13.60}$$

- The spectrum $F(\omega, \theta)$ is the Fourier transform of the wave form $f(t, \theta)$. The wave form is observed directly at the origin of the coordinate system (see Sec. 13.2.2.1).
- The exponential term describes the delay of the plane wave from the origin to the position $\boldsymbol{x}'$ of the monopole. It can be realized by a time delay of the wave form $f(t, \theta)$.
- The high-pass frequency response $K(\omega)$ combines the term $H(\omega)$ from the approximation of a line source by a point source in Eq. 13.33 and the effect of the differentiation in Eq. 13.58

$$K(\omega) = \sqrt{\frac{\omega}{c}}\, e^{j3\pi/4}\,. \tag{13.61}$$

  It can be realized by filtering the wave form $f(t, \theta)$.
- The amplitude modification $A(\|\boldsymbol{x} - \boldsymbol{x}'\|)$ comes from the approximation of a line source by a point source in Eq. 13.34. It is discussed in detail in Sec. 13.3.6.3.

Finally, the driving signals for a wave field that is composed of various plane waves are obtained by superposition of the individual plane wave driving signals D_θ

$$D(\omega, \boldsymbol{x}|\boldsymbol{x}') = \int_0^{2\pi} D_\theta(\omega, \boldsymbol{x}|\boldsymbol{x}')\, d\theta\,. \tag{13.62}$$

13.3.6.3 Independence of the Driving Signals from the Listener Position

The driving signals for a plane wave in Eq. 13.59 or for a wave field composed of plane waves in Eq. 13.62 formally depend on time t or frequency ω, the loudspeaker position $\boldsymbol{x}'$ on the contour ∂L and on the listener position $\boldsymbol{x}$ within the area L. Time dependence is a necessary feature, dependence on the loudspeaker position is manageable by multichannel filtering, but dependence on the position of a listener is highly undesirable. Even if the position of a listener was known at all times, e.g. by a tracking system, this would not solve the problem of sound reproduction for multiple listeners in a larger audience.

Fortunately, the dependence on the listener position is rather mild and is not at all comparable with the well-known sweet spot limitation of stereophonic systems. The only component of $D_\theta(\omega, \boldsymbol{x}|\boldsymbol{x}')$ which depends on $\boldsymbol{x}$ is the amplitude modification $A(\|\boldsymbol{x} - \boldsymbol{x}'\|)$ due to the approximation of the line sources. A less drastic approximation, e.g. by multiple point sources, would result in less amplitude modification. However, most important, all the other components of $D_\theta(\omega, \boldsymbol{x}|\boldsymbol{x}')$ do not depend on the listener position at all. Delay and filtering of the wave form are correct for the total area L.

For practical realizations, the amplitude correction is set to a fixed listener position $A(\|\boldsymbol{x}_0 - \boldsymbol{x}'\|)$. Then the resulting modified driving signals $D_{0,\theta}$ are independent of the listener position $\boldsymbol{x}$

$$D_{0,\theta}(\omega, \boldsymbol{x}') = D_\theta(\omega, \boldsymbol{x}_0|\boldsymbol{x}') \; . \tag{13.63}$$

They cause a slight deviation in the reproduction volume, but delay and filtering operations remain unaffected. The amount of this deviation and its spatial distribution can be controlled by suitable choice of $\boldsymbol{x}_0$ [18].

13.3.7 Signal Processing Structure

Now that the driving signals for the loudspeakers are determined, the signal processing structure for their production is investigated. From now on, only the listener independent driving signals $D_{0,\theta}(\omega, \boldsymbol{x}')$ are used. They are the output of a signal processing chain with the wave forms $F(\omega, \theta)$ of the plain wave components as input. In short form this processing chain is written as

$$D_{0,\theta}(\omega, \boldsymbol{x}') = M(\omega, \boldsymbol{x}', \theta)\, F(\omega, \theta) \tag{13.64}$$

with

$$M(\omega, \boldsymbol{x}', \theta) = 2w(\boldsymbol{x}', \theta)\, A\big(\|\boldsymbol{x}_0 - \boldsymbol{x}'\|\big)\, K(\omega)\; e^{j\frac{\omega}{c}\langle \boldsymbol{x}', \boldsymbol{n}_\theta \rangle} \; . \tag{13.65}$$

Complex wave fields can be represented by a superposition of plane waves as shown in Eq. 13.62. In practical spatial reproduction systems the number

of plane wave components is limited. Then the driving signals contain contributions from a finite number of plane waves from a discrete set of angles denoted by θ_m with $m = 1, 2, \ldots$

$$D_0(\omega, \boldsymbol{x}') = \sum_m D_{0,\theta_m}(\omega, \boldsymbol{x}') = \sum_m M(\omega, \boldsymbol{x}', \theta_m)\, F(\omega, \theta_m)\,. \tag{13.66}$$

Furthermore, from this finite number of plane wave components, driving signals for each discrete loudspeaker position $\boldsymbol{x}'_n$ have to be generated. The resulting structure is best formulated in vector notation with

$$\boldsymbol{D}_0(\omega) = \begin{bmatrix} \vdots \\ D_0(\omega, \boldsymbol{x}'_n) \\ \vdots \end{bmatrix}\,, \qquad \boldsymbol{F}(\omega) = \begin{bmatrix} \vdots \\ F(\omega, \theta_m) \\ \vdots \end{bmatrix}\,, \tag{13.67}$$

$$\boldsymbol{M}(\omega) = \begin{bmatrix} \vdots \\ \ldots\, M(\omega, \boldsymbol{x}'_n, \theta_m)\, \ldots \\ \vdots \end{bmatrix}\,. \tag{13.68}$$

Then the vector of driving signals for each loudspeaker is calculated from the vector of wave forms for each plane wave component by

$$\boldsymbol{D}_0(\omega) = \boldsymbol{M}(\omega)\, \boldsymbol{F}(\omega)\,. \tag{13.69}$$

In the time domain the driving signals are the result of a multichannel convolution

$$\boldsymbol{d}_0(t) = \boldsymbol{m}(t) * \boldsymbol{f}(t)\,. \tag{13.70}$$

In short, the signal processing structure for the calculation of the loudspeaker driving signals is a multiple-input, multiple-output (MIMO) system which performs a multichannel convolution with the wave forms of the plane wave components. The convolution filters comprise various operations in time and space as discussed in Sec. 13.3.6.2 and 13.3.6.3.

13.4 Implementation of a Wave Field Synthesis System

Finally, the implementation of a wave field synthesis system is shown by an example. Fig. 13.9 sketches a typical configuration of a virtual acoustical scene. The grey background shows the floor plan of a church with the apsis on the right. Here a singer or a musician is placed as a primary sound source. Its sound waves propagate through the church via a direct path and multiple reflections (indicated by dashed lines). The intention is now to reproduce the sound field in the center part of the church by a wave field synthesis system installed at a remote location. To this end, the sound waves arriving at the

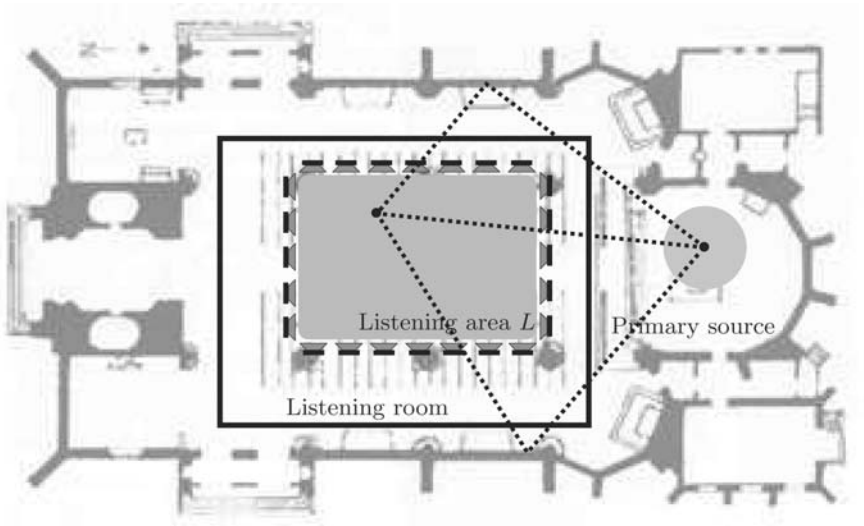

Fig. 13.9. Reproduction of a virtual environment with a wave field system.

boundary of the listening area serve as source signals for the loudspeakers of the wave field synthesis system.

There are different ways to obtain these loudspeaker signals corresponding to model based and data based rendering techniques (see Sec. 13.3.6). In this example, a virtual scene model based on a decomposition into plane waves is used for simplicity. For more advanced approaches using data based rendering see e.g. [12, 21].

The acoustical scene inside the church can be simplified e.g. by an image source model. It starts from a point source model for the primary source in the apsis and approximates the reflections by sources mirrored on the reflecting surfaces. The total sound field is then represented by a multitude of point sources. Each of these point sources can be decomposed into a superposition of plane waves. The directions for two selected reflections to an arbitrary listener position are indicated by the dashed lines in Fig. 13.9. Varying the secondary source position along the boundary ∂L of the listening area gives the normal directions $\boldsymbol{n}_\theta$ for the determination of the driving signals e.g. in Eqs. 13.59 and 13.60. Playing back the driving signals with a wave field installation in a remote listening room (indicated by the solid line in Fig. 13.9) then reproduces the sound field within the listening area.

An implementation of a wave field synthesis system with a circular loudspeaker array is shown in Fig. 13.10. Here the planar area L is a disc with a radius of 1.5 m. A total of 48 two-way loudspeakers are mounted on the circumference ∂L with a spacing of about 20 cm. The analog driving signals are delivered by three 16-channel audio amplifiers with digital inputs shown in Fig. 13.11. The digital input signals are the result of the multichannel convo-

lution (Eq. 13.70). It is realized by fast convolution techniques in real-time on a personal computer. The system described here is located at the Telecommunications Laboratory (Multimedia Communications and Signal Processing) of the University of Erlangen-Nuremberg in Germany [13].

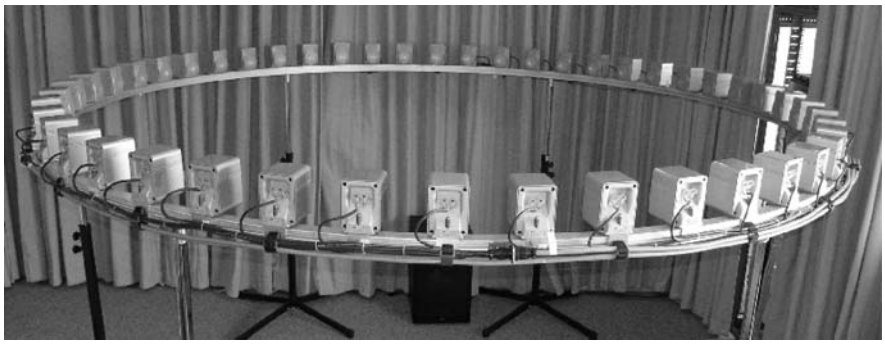

Fig. 13.10. Circular loudspeaker array with a radius of 1.5 m and 48 channels.

Fig. 13.11. Three 16-channel audio amplifiers for the array in Fig. 13.10 mounted in a 19 inch rack.

13.5 Conclusions

This chapter has given an introduction to wave field synthesis. It is based on the acoustic wave equation and the representation of its solutions by plane waves and Green's functions. Starting from these physical foundations, it has been shown how to derive the driving signals for the loudspeaker array of the resulting wave field synthesis systems.

The derivation is valid for rather general geometries and sizes of loudspeaker arrays. Furthermore, no assumption on the position of the listener is required. Then the reproduced sound field is physically correct within the limitations imposed by amplitude deviation and by spatial discretization effects. The computation of the loudspeaker driving signals is conceptually simple and is performed by a multichannel convolution. In short, the realizing technique of wave field synthesis systems is obtained by mapping the acoustic wave equation to a multiple-input, multiple-output system (MIMO) system.

However, the practical realization of wave field synthesis has some pitfalls, which can be avoided by further signal processing techniques. These pertain the simplified monopole model of the loudspeakers and the acoustical reflections of the loudspeakers within the listening room.

So far it has been assumed that acoustical monopoles can be approximated well by small loudspeakers with closed enclosures. If required, this approximation can be improved with digital compensation of non-ideal loudspeaker properties [20]. The second pitfall consists of the reflections of the loudspeaker array signals in the listening room. They may degrade the performance level predicted from theory. Countermeasures are passive or active cancellation of these reflections. Especially, active cancellation seems promising by using the loudspeaker arrays for reproduction also for the cancellation of room reflections [19].

The presentation here has been focussed on the determination of the driving signals, once a representation of an existing or virtual sound field is given in terms of plane waves. Such a representation is always possible through the so-called plane wave decomposition [12]. How to obtain this decomposition from microphone array measurements in a real room belongs to the area of wave field analysis. This area has not been discussed here in detail. For more information see e.g. [12, 21]. Also not discussed here were the relations of wave field synthesis to other spatial reproduction techniques. For a comparison with Ambisonics see [15].

References

[1] M. Abramowitz, I.A. Stegun: *Handbook of Mathematical Functions,* New York, NY, USA: Dover Publications, 1972.

[2] G.B. Arfken, H.J. Weber: *Mathematical Methods for Physicists,* 5th ed., San Diego, CA, USA: Academic Press, 2001.

[3] A.J. Berkhout: A holographic approach to acoustic control, *Journal of the Audio Engineering Society,* **36**, 977–995, December 1988.

[4] R.N. Bracewell: *Fourier Analysis and Imaging,* Boston, MA, USA: Kluwer, 2003.

[5] S. Brix, T. Sporer, J. Plogsties: CARROUSO - An European approach to 3D-audio, *110th AES Convention,* Audio Engineering Society (AES), Amsterdam, Netherlands, May 2001.

[6] W. de Bruin: *Application of wave field synthesis in videoconferencing,* PhD thesis, Delft University of Technology, 2004.
[7] J. Coleman: Ping-pong sample times on a linear array halve the Nyquist rate, *Proc. ICASSP '04*, **4**, 925–928, Montreal, Canada, 2004.
[8] J.D. Gaskill: *Linear Systems, Fourier Transforms, and Optics,* New York, NY, USA: Wiley, 1978.
[9] I.S. Gradshteyn, I.M. Ryzhik: *Tables of Integrals, Series, and Products,* San Diego, CA, USA: Academic Press, 1965.
[10] S. Hassani: *Mathematical Physics, A Modern Introduction to its Foundations,* Berlin, Germany: Springer, 1999.
[11] E. Hulsebos: *Auralization using Wave Field Synthesis,* PhD thesis, Delft University of Technology, 2004.
[12] E. Hulsebos, D. de Vries, E. Bourdillat: Improved microphone array configurations for auralization of sound fields by wave field synthesis, *Journal of the Audio Engineering Society (AES),* **50**(10), 779–790, Oct. 2002.
[13] Chair of Multimedia Communications and Signal Processing, University Erlangen-Nuremberg, Germany, `http://www.lnt.de/LMS`.
[14] P.M. Morse, H. Feshbach: *Methods of Theoretical Physics – Part I,* New York, NY, USA: McGraw-Hill, 1953.
[15] R. Nicol, M. Emerit: Reproducing 3D-sound for videoconferencing: A comparison between holophony and ambisonic, *Proc. DAFX '98*, Barcelona, Spain, Nov. 1998.
[16] A.D. Pierce: *Acoustics – An Introduction to its Physical Principles and Applications,* Acoustical Society of America, 1991.
[17] R. Rabenstein, P. Steffen, S. Spors: Representation of two-dimensional wave fields by multidimensional signals, *Signal Processing,* to be published.
[18] J.-J. Sonke, D. de Vries, J. Labeeuw: Variable acoustics by wave field synthesis: A closer look at amplitude effects, *Proc. 104th AES Convention,* prepr. 4712, Audio Engineering Society (AES), Amsterdam, Netherlands, May 1998.
[19] S. Spors, H. Buchner, R. Rabenstein: Adaptive listening room compensation for spatial audio systems, *Proc. EUSIPCO '04,* 1381–1385, Vienna, Austria, 2004.
[20] S. Spors, D. Seuberth, R. Rabenstein: Multiexciter panel compensation for wave field synthesis, *Proc. DAGA '05,* Munich, Germany, 2005.
[21] S. Spors, H. Teutsch, A. Kuntz, R. Rabenstein: Sound field synthesis, in Y.Huang and J.Benesty (eds.), *Audio Signal Processing for Next-Generation Multimedia Communication Systems,* Boston, MA, USA: Kluwer, 2004.
[22] E.W. Start: *Direct Sound Enhancement by Wave Field Synthesis,* PhD thesis, Delft University of Technology, 1997.
[23] E.N.G. Verheijen: *Sound Reproduction by Wave Field Synthesis,* PhD thesis, Delft University of Technology, 1997.

[24] P. Vogel: *Application of Wave Field Synthesis in Room Acoustics,* PhD thesis, Delft University of Technology, 1993.

[25] D. de Vries, E.W. Start, V.G. Valstar: The wave field synthesis concept applied to sound reinforcement: Restrictions and solutions, *96th AES Convention,* Audio Engineering Society (AES), Amsterdam, Netherlands, February 1994.

[26] E.G. Williams: *Fourier Acoustics: Sound Radiation and Nearfield Acoustical Holography,* San Diego, CA, USA: Academic Press, 1999.